J. Fluid Mech. (1966), *vol.* 26, *part* 2, *pp.* 281–307
Printed in Great Britain

An experimental investigation of the instability of an incompressible, separated shear layer

By F. K. BROWAND

Department of Aeronautics and Astronautics, Massachusetts Institute of Technology, Cambridge, Massachusetts

(Received 6 January 1966)

The investigation of a separated shear layer was undertaken to clarify the non-linear mechanisms associated with instability and transition to turbulence. Such an investigation is of practical importance since profiles which resemble the separated shear layer are a common occurrence.

A two-dimensional free shear layer was formed by separation of a laminar boundary layer from a rearward-facing step. The free-stream speed was approximately 16 ft./sec. Hot-wire measurements were made in the region directly downstream of the plate trailing edge. The measurements included mean velocity profiles, frequency spectra of the longitudinal fluctuation, and root-mean-square amplitude and phase distributions of various spectral components of the longitudinal fluctuation. Several measurements were designed to detect the presence of periodic spanwise structure.

The most important findings were:

(i) Significant non-linear distortion of the initial unstable wave occurred without periodic spanwise structure.

(ii) Non-linear distortion was first manifest by the growth of a subharmonic oscillation, which was strongly intermittent. Numerous harmonics of the subharmonic oscillation were also present.

(iii) Strong evidence suggests that secondary instabilities were present, which created still higher frequencies.

1. Introduction

Klebanoff, Tidstrom & Sargent (1962) have performed a very significant experiment dealing with the later stages of boundary-layer instability and transition to turbulence. They found that the most unstable wave as predicted by two-dimensional, linear stability theory in reality contained nearly periodic spanwise variations in amplitude. These amplitude variations resulted in streamwise vorticity which caused instantaneous velocity profiles with inflexion points to form at various spanwise locations. A high-frequency breakdown was observed to occur at these inflexion points.

Benney (1961) performed a non-linear analysis, assuming the existence of both two-dimensional and three-dimensional waves. He showed the existence of streamwise vorticity and warping of spanwise profiles—features which agreed remarkably well with the experimental work.

Greenspan & Benney (1963) modelled the high-frequency breakdown with an unsteady, inflexion-point flow. It was concluded, in basic agreement with experiment, that the most amplified wave was approximately the one associated with a free shear layer of appropriate dimension, and that the wave amplitude could increase very rapidly.

In spite of these comforting correspondences between experiment and theory, there is a strong suspicion that transition in unbounded flows does not occur in the manner prescribed above. That is, three-dimensional effects appear to be far less important in the initial distortion of the primary oscillation. Also, the 'bursting' nature of the secondary breakdown in boundary-layer transition is not observed in the transition of wake-type flows. Some important investigations which led to these conclusions have been Sato (1956, 1959, 1960), Sato & Sakao (1964), Sato & Kuriki (1961), for the separated shear layer, the two-dimensional jet, and the flat-plate wake; and also Roshko (1954), Tritton (1959), and Bloor (1964), all of which were investigations of the flow behind a circular cylinder.

Of the unbounded flows, the separated shear layer has received the least attention experimentally. However, there is a large body of theoretical work which is pertinent. The simplest theoretical studies date to Rayleigh (1896). Most of the early theoretical work was for inviscid flow, and Foote & Lin (1950) showed that inviscid theory was a good approximation for unbounded flows at large Reynolds numbers. Esch (1957) summarized earlier work and looked at a shear profile composed of three straight-line segments when viscosity was present. Tatsumi & Gotoh (1960) showed that all parallel flows with a velocity difference at $y = \pm\infty$ possess no critical Reynolds number. Lessen & Fox (1955) have calculated the eigenvalues (at $R = \infty$) for the similarity profile produced between two parallel streams of different velocity. (The similar solution was determined by Locke (1951) and Lin (1953).) Drazin & Howard (1962) have also investigated profiles approximating the free shear layer. Michalke (1964) has calculated eigenvalues and eigenfunctions for the hyperbolic tangent profile in the inviscid limit, and Betchov & Szewczyk (1963) have determined the neutral curve and curves of constant amplification as a function of Reynolds number. Michalke (1965) and Schade (1964) have considered various non-linear aspects of the wave growth. Most recently, Michalke (1966) has considered the spatial amplification of disturbances for a hyperbolic tangent profile; and Kelly (1965) investigated the problem of subharmonic resonance.

An experimental investigation of the instability of an incompressible, separated shear layer (initially two-dimensional) was undertaken with the following specific points in mind: (*a*) investigation of the region further downstream where non-linear effects are abundant; (*b*) the mechanism of energy transfer from a single frequency to a complete (turbulent) spectrum of frequencies; (*c*) importance of three-dimensional structure in the initial stages of non-linear growth.

2. Description of experiment.

The experimental work was performed in a small, open return wind tunnel having a contraction ratio of 36 : 1. The longitudinal turbulence level in the free stream measured 0·12% at 16 ft./sec, and somewhat less at higher speeds.

Observation of hot-wire traces indicated that low-frequency unsteadiness represented the bulk of the longitudinal fluctuation.

The free shear layer was formed by the separation of a boundary-layer flow

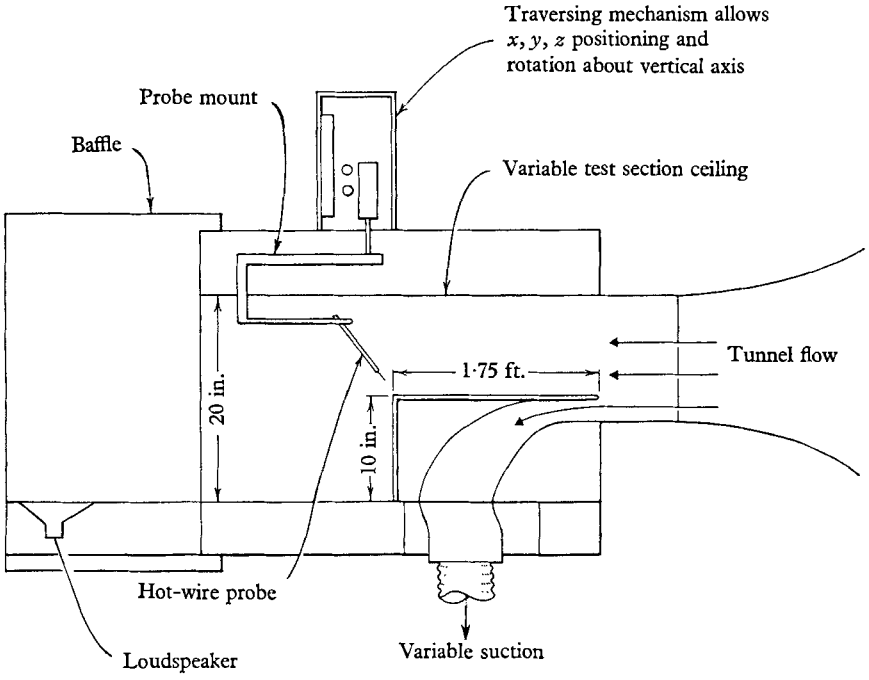

FIGURE 1. Sketch of working area for free shear layer experiments (not to scale).

from a rearward-facing step, figure 1. The step completely spanned the width of the test section (1 ft.), and the flow should be approximately two-dimensional in the central 6 in. By observing the shedding frequency behind a small cylindrical rod placed in the stream, the velocity above the plate trailing edge was fixed at 15·8 ft./sec. The tunnel speed fluctuated slowly over a period of time owing to variations in the motor r.p.m. The time variations in the main stream were kept within $\pm$ 0·4 ft./sec by periodic adjustment.

In order to keep the flat-plate boundary layer free of oscillations before separation at the plate trailing edge, the plate length was fixed by the requirement that the critical Reynolds number of the boundary layer should not be exceeded. To prevent separation at the leading edge (and hence transition on the plate), the air below the plate had to be removed with the help of suction (figure 1).

Hot-wire measurements were made in the downstream region within 4 in. of the plate trailing edge, which corresponded to about three wavelengths of the primary oscillation. In this distance the shear layer had increased in thickness from about $\frac{1}{4}$ in. to about $1\frac{1}{2}$ in.

Mean velocities were measured at several downstream stations by traversing the hot wire vertically through the shear layer. The frequency content of the longitudinal fluctuation in the range from 20 c/s to 300 c/s was determined with the aid of a narrow-band wave analyser. (The frequency of the primary oscillation was 79 c/s.) The root-mean-square amplitude distributions (and, in some cases, the phase distributions) of various significant frequency components were measured as a function of the vertical co-ordinate. This provided sufficient information to calculate the form of the instantaneous fluctuation at several locations. Measurements to indicate three-dimensionality included the determination of mean velocity profiles at various spanwise stations, recording the variation of the longitudinal fluctuation in the spanwise direction, and a determination of the phase of the primary oscillation in the spanwise direction. In most instances, an x–y plotter was used to obtain continuous variations.

It is common practice, in observing instabilities in parallel flows, to fix the frequency and phase of the disturbance by excitation. The reason is that, by artificially producing a disturbance (nearly) coinciding in frequency with the disturbance which would grow 'naturally', one is able to 'lock in' the oscillation and obtain amplitudes which are much more steady and measurable. There is no *a priori* justification for the assumption that the instability process will be the same as would occur if the flow were allowed to develop naturally. Therefore, it is necessary to establish experimentally the relationship between the naturally excited flow and the externally excited flow. Two complete sets of measurements were made in the separated shear layer to determine the differences, if any, in the process of instability when excitation was present. One set of measurements was taken with no external excitation, and will be referred to as 'natural instability' or 'natural transition'. A second set of measurements was taken while the shear layer was being excited by a loudspeaker placed at the rear of the test section. The frequency of excitation was 90 c/s—about 10 % above that frequency which predominated in the natural instability. The amplitude of the excitation, measured with a Bruel–Kiaer condenser microphone, was about 14 dB (sound pressure level) above the background noise.

Several length and velocity scales are used to non-dimensionalize the results. The vertical co-ordinate, y (measured positive upwards from the plane of the plate), is non-dimensionalized by the momentum thickness

$$\theta = \int_{-\infty}^{\infty} \frac{U}{U_\delta}\left(1-\frac{U}{U_\delta}\right) dy,$$

where U_δ is the velocity at the outer edge of the shear layer. Both θ and U_δ are functions of x. The longitudinal co-ordinate, x (measured positive downstream from the plate trailing edge), and the spanwise co-ordinate z, are measured in units of λ, the wavelength of the forced oscillation. The experimentally determined value is $\lambda = 1{\cdot}25 \pm 0{\cdot}25$ in. For the purpose of non-dimensionalizing, λ will be taken as a constant equal to 1·25 in. U_0 refers to the tunnel speed, which is constant and equal to 15·8 ft./sec.

3. Experimental results

3.1. *The nature of the instability with and without forcing*

The first important observation is that the qualitative character of the instability process is the same with or without forcing. This result justifies the use of the forcing oscillation, which provides much more sharply defined fluctuations, to investigate the process of instability. The results presented here were obtained from data taken with forcing present; some results without forcing will also be included to illustrate the similarities.

3.2. *Mean velocity*

In figure 2 (*a*), (*b*), the mean velocity profiles are presented for nine values of x/λ. The most interesting feature is the appearance of a small local maximum in the mean shear at about $x = 0{\cdot}8\lambda$. At $x = 3{\cdot}2\lambda$ the local maximum has disappeared. The generation of a second inflexion point in the mean profile was readily apparent, largely because of the continuous recording technique.

Figure 3 gives the value of the maximum mean shear as a function of x/λ, and figure 4 gives the growth of the momentum thickness and momentum-thickness Reynolds number with x/λ. It will be seen that the maximum shear suffers a large decrease coincident with the appearance of the secondary inflexion point in the mean profile. Also, the rate of change of the momentum thickness increases markedly at about $x = 0{\cdot}8\lambda$.

The mean velocity profiles are plotted in non-dimensional form in figure 5 (*a*), (*b*). Two curves are presented for comparison. The solid curve in 5 (*a*), (*b*), is the similarity solution calculated by Lin (1953) for incompressible flow. The dotted curve in 5 (*b*) is an experimental turbulent profile measured by Liepmann & Laufer (1947). (At each value of x, the non-dimensional profiles were shifted an increment in y/θ to make the point, $y/\theta = 0$, correspond to $U/U_\delta = 0{\cdot}5$. Figure 6 gives the values of y/θ which are the locus of $U/U_\delta = 0{\cdot}5$.) In the early stages of shear-layer growth (figure 5 (*a*)), the profile is changing from the boundary-layer flow. A similarity seems to be established at about $x = 0{\cdot}8\lambda$; but it is quite clear that the experimental profiles have larger mean shear than the laminar similar solution predicts. This is evidently due to the growth of the unstable oscillation(s). At $x = 3{\cdot}2\lambda$, the mean profile exhibits a tendency to depart from the previously established similarity, and has begun to move towards turbulent similarity.

The discrepancy between experiment and theory at large negative values of y/θ is also interesting. There seems to be no reason to doubt the experimental values in this region. The hot wire was free from buoyancy effects above about 0·3 ft./sec. Any errors produced by rectifying effects at low velocities do not seem to be of sufficient magnitude to correct the discrepancy. The hot wire responds to the absolute magnitude of the velocity in the (x, y)-plane, so, strictly speaking, the vertical component of the mean velocity should be subtracted from the experimental data. However, the vertical component theoretically determined by Locke (1951) can be shown to produce an insignificant correction in the region of interest.

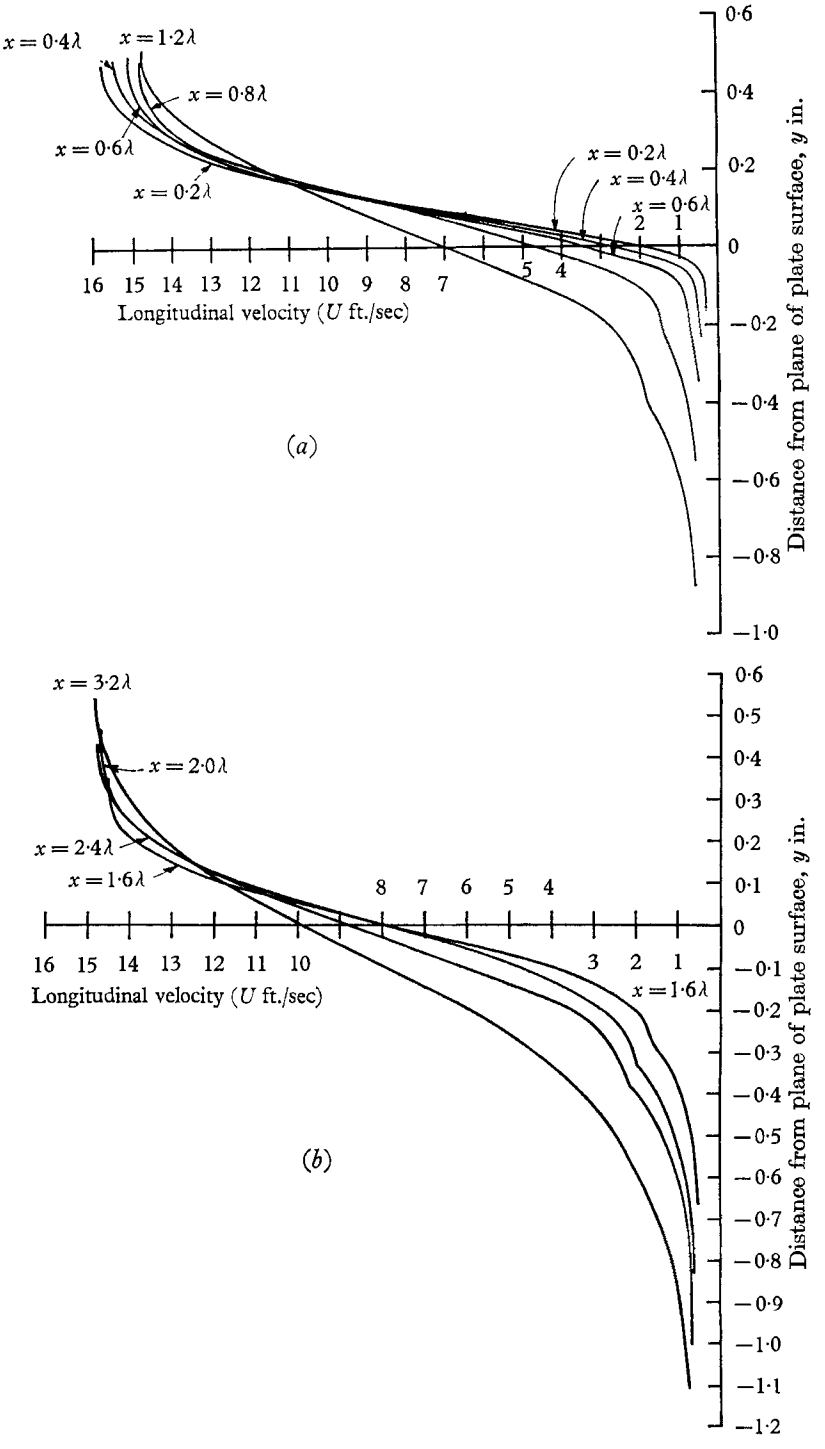

FIGURE 2. (*a*), (*b*). Mean velocity profiles at different distances downstream of plate trailing edge.

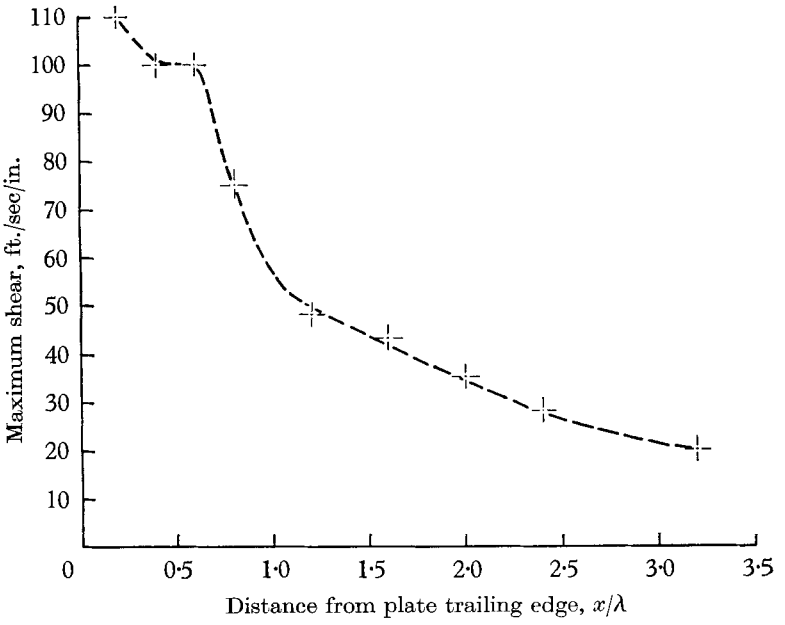

FIGURE 3. Maximum value of mean shear at various downstream positions.

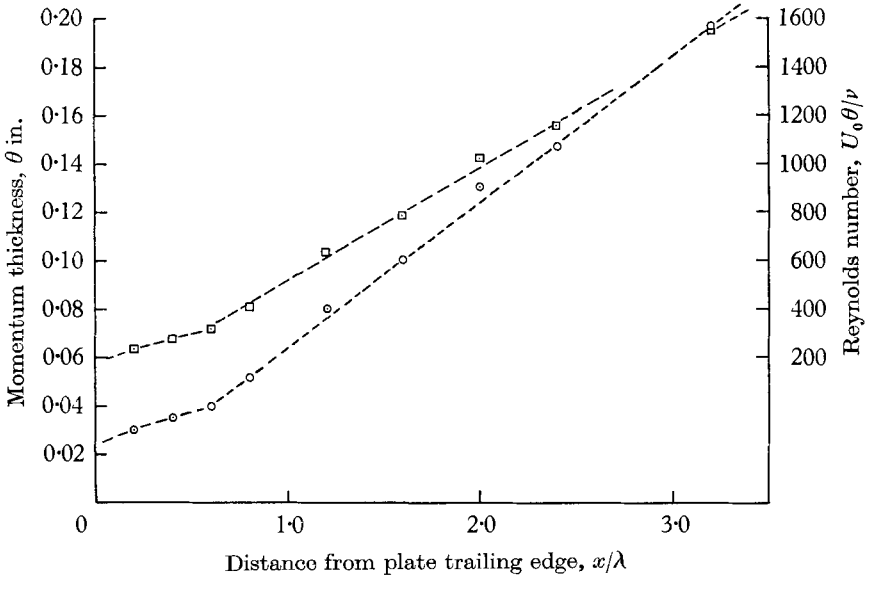

FIGURE 4. ⊙, Momentum thickness, θ; and ⊡, momentum-thickness Reynolds number $U_0\theta/\nu$ as a function of downstream position

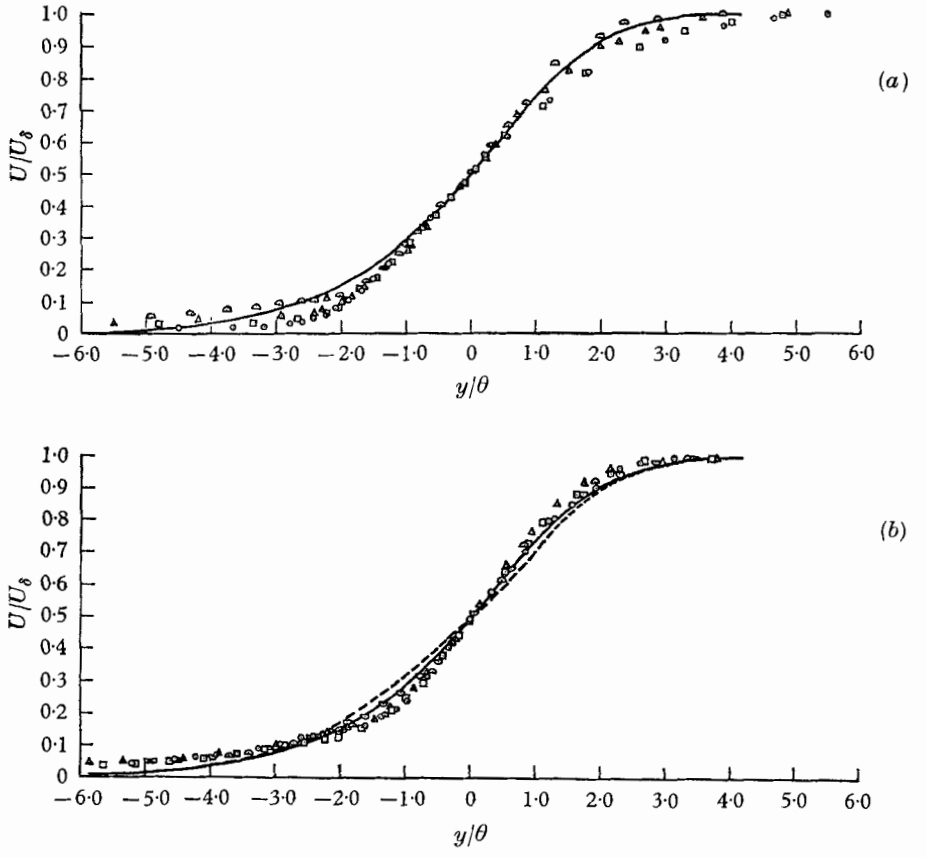

FIGURE 5. Non-dimensional mean velocity profiles at different downstream positions. ——, Lin (1953), laminar similarity; – – –, Liepmann–Laufer (1947), turbulent experimental. (*a*) ⊙, $x = 0{\cdot}2\lambda$; ⊡, $x = 0{\cdot}4\lambda$; △, $x = 0{\cdot}6\lambda$; ◠, $x = 0{\cdot}8\lambda$. (*b*) ⊙, $x = 1{\cdot}2\lambda$; ⊡, $x = 1{\cdot}6\lambda$; △, $x = 2{\cdot}0\lambda$; ◠, $x = 2{\cdot}4\lambda$; ◡, $x = 3{\cdot}2\lambda$.

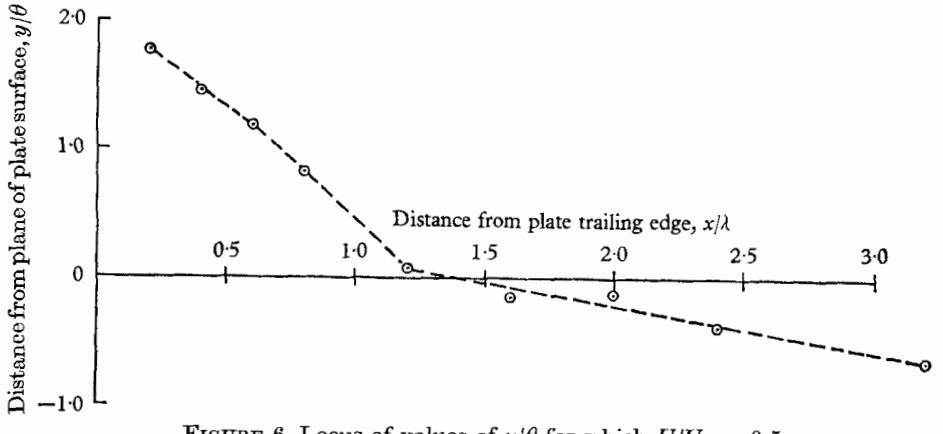

FIGURE 6. Locus of values of y/θ for which $U/U_\delta = 0{\cdot}5$.

3.3. *Spectra*

Although some 45 separate spectra were recorded in the shear layer, only a representative portion will be reproduced. Figure 7 (*a*), (*b*), and (*c*) presents

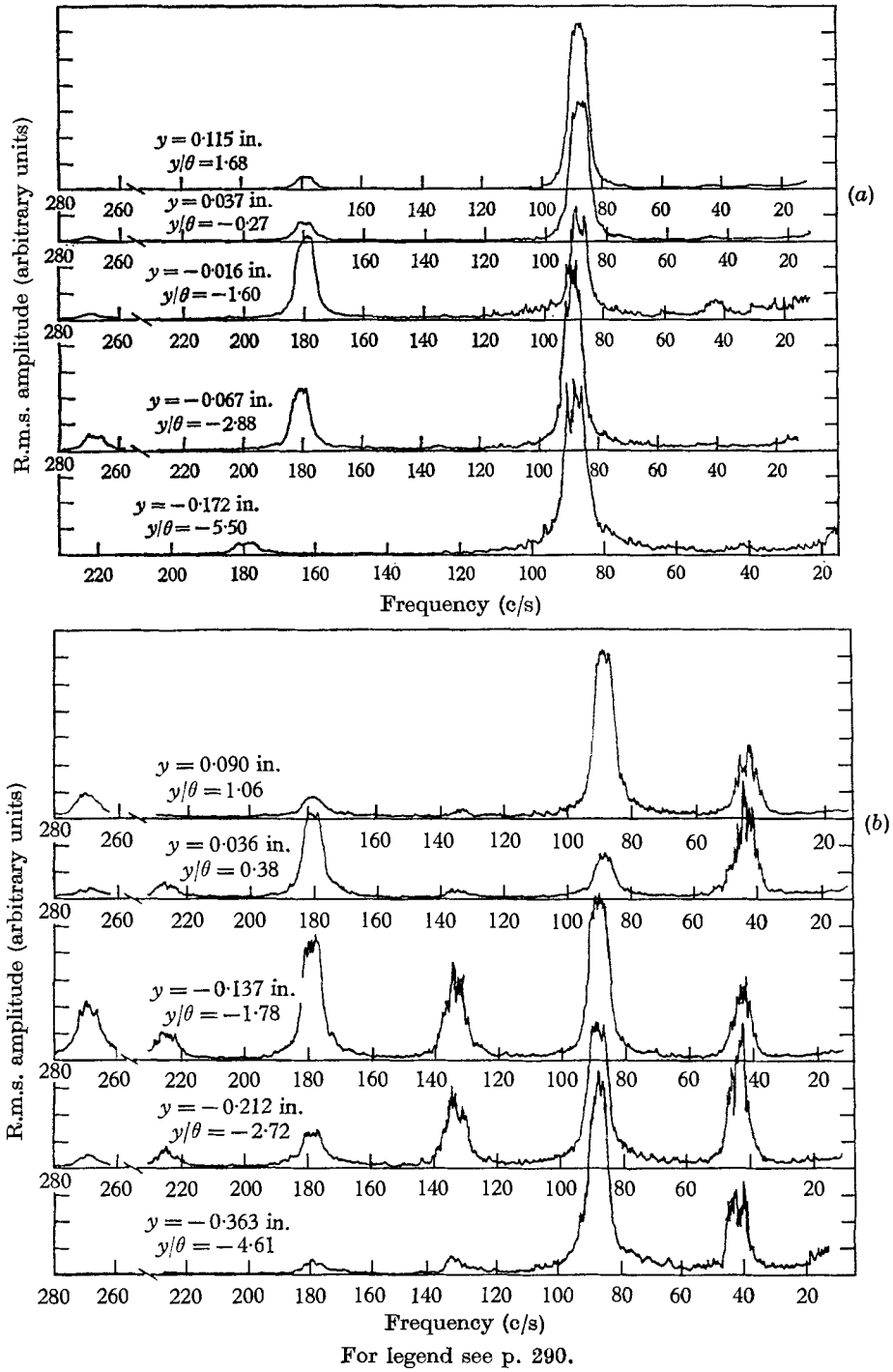

For legend see p. 290.

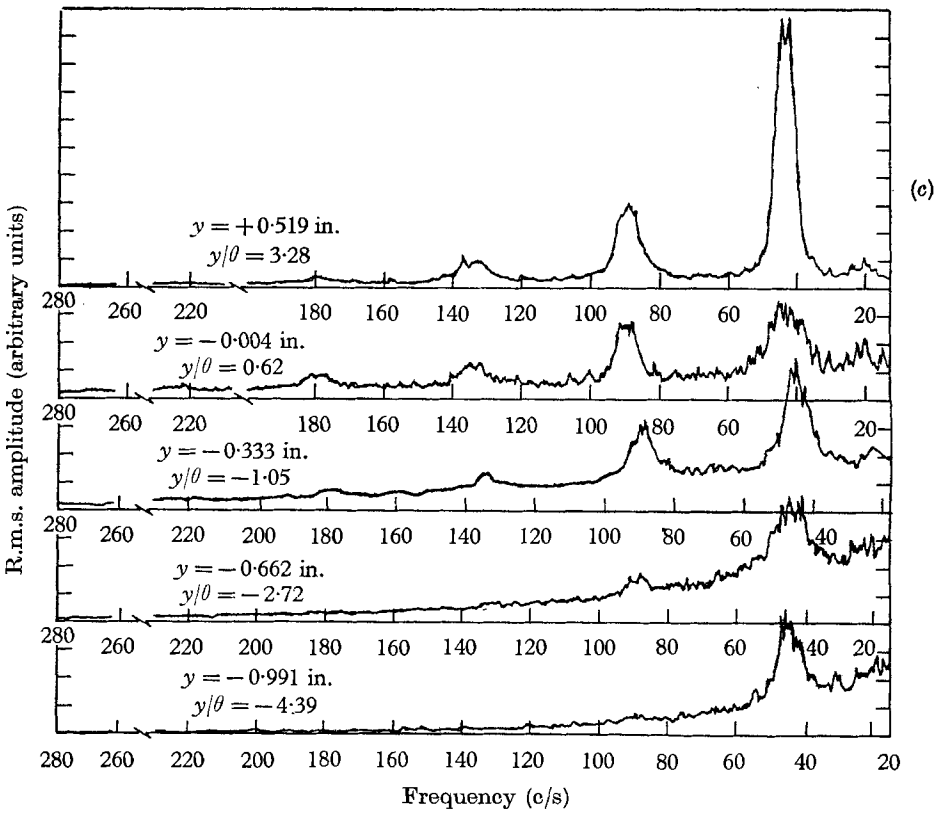

FIGURE 7. Frequency spectra at different values of y (forcing frequency, 90 c/s) for (*a*) $x = 0{\cdot}6\lambda$; (*b*) $x = 1{\cdot}2\lambda$; (*c*) $x = 3{\cdot}2\lambda$.

five spectra for values of x equal to $0{\cdot}6\lambda$, $1{\cdot}2\lambda$, and $3{\cdot}2\lambda$, respectively. These spectra are traces of the actual, unreduced data. The amplitudes of components at different values of y cannot be compared since the hot-wire gain is not constant, but the relative amplitudes of harmonic components at the same value of y are (approximately) correct.

At $x = 0{\cdot}6\lambda$ (figure 7 (*a*)), one observes a discrete spectrum composed of the component at the forcing frequency, 90 c/s (henceforth called the primary oscillation), and its two higher harmonics. At $x = 1{\cdot}2\lambda$ (figure 7 (*b*)), a remarkable effect is observed. The spectrum is still discrete; but, beside the primary oscillation and its harmonics, a subharmonic component and harmonics of the subharmonic now appear. In fact, the subharmonic is present to a lesser degree at $x = 0{\cdot}8\lambda$, and its birth seems to coincide with the generation of the secondary inflexion point in the mean profile. (Subharmonic growth has been observed by other investigators, e.g. Sato (1959) and Wehrmann & Wille (1958).)

It must be stressed that the appearance of the subharmonic oscillation is not the result of the forcing. Figure 8 (*a*), (*b*), shows spectra which were recorded when no forcing oscillation was present. At $x = 1{\cdot}2\lambda$, the naturally excited primary oscillation (79 c/s) is observed; and, at $x = 2{\cdot}4\lambda$, the subharmonic response is very

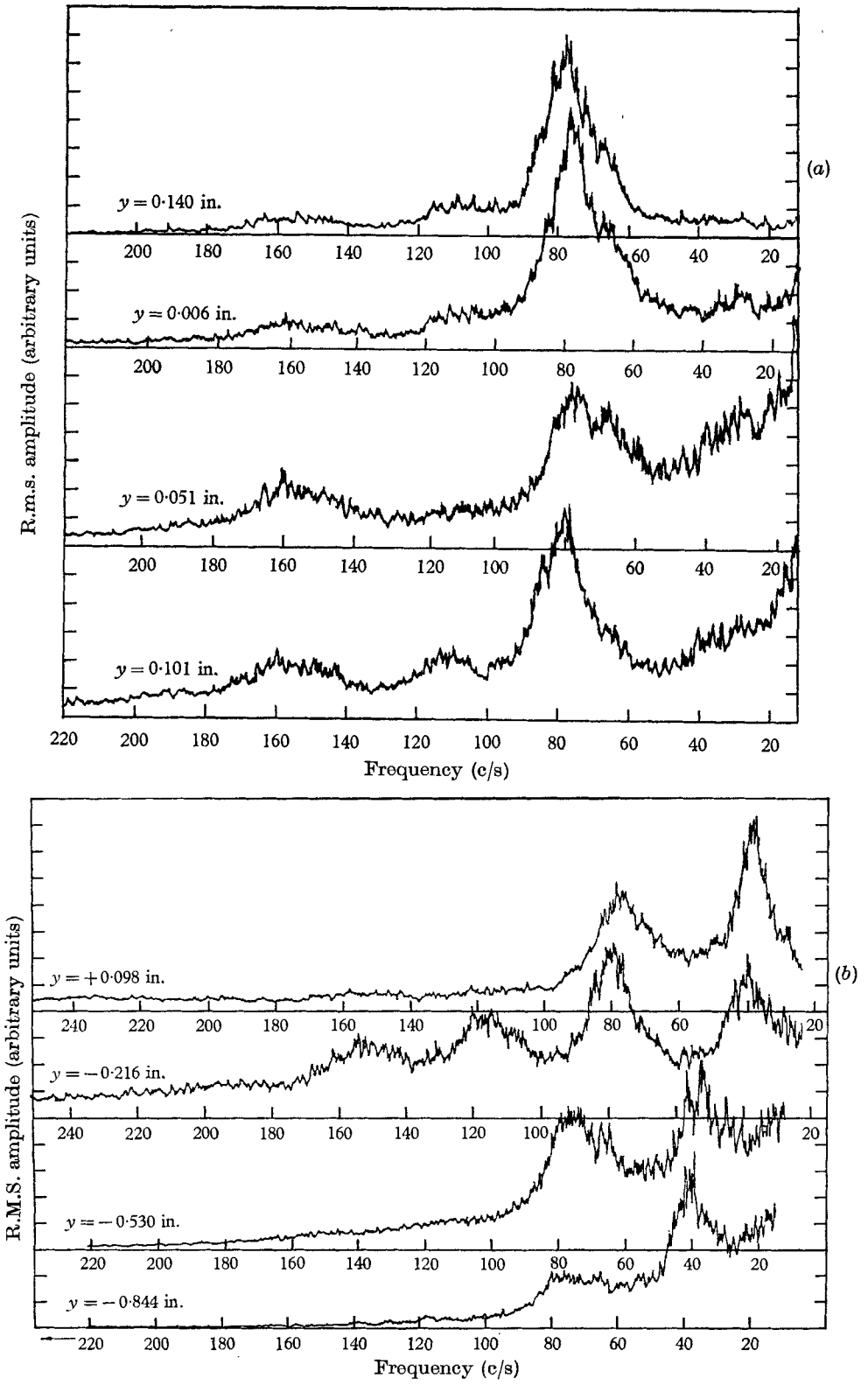

FIGURE 8. Frequency spectra at different values of y (natural transition) for (*a*) $x = 1{\cdot}2\lambda$; (*b*) $x = 2{\cdot}4\lambda$.

much in evidence. The peaks are not nearly as sharp as with the forcing present, and the process is shifted downstream; but the harmonic content is similar. The generation of a harmonic frequency spectrum which includes the subharmonic is also found at other tunnel speeds. Figure 9 is a single spectrum recorded in the shear layer at a tunnel speed of 24·5 ft./sec. The forcing frequency in this case is 200 c/s. One must conclude that the generation of such a frequency spectrum is unquestionably an inherent part of the process of free shear-layer instability.

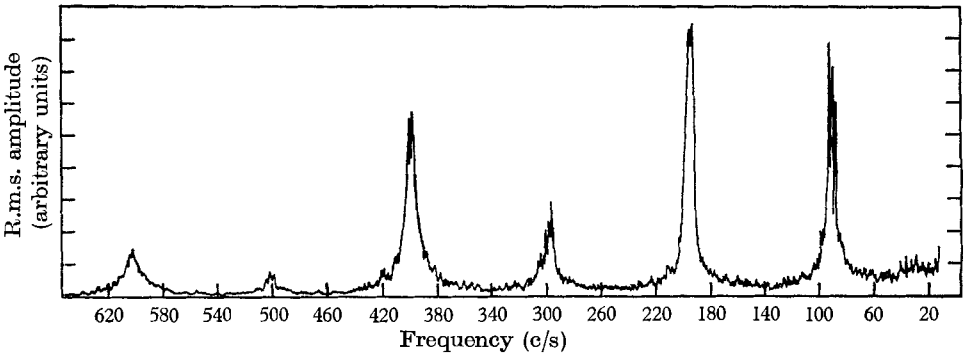

FIGURE 9. Frequency spectrum at tunnel speed, $U_0 = 24{\cdot}5$ ft./sec (forcing frequency, 200 c/s).

Several other effects can be observed in figure 7 (*a*), (*b*), and (*c*). First is the tendency towards a smoothing or 'filling in' of the frequency spectrum as one proceeds downstream. This is especially obvious in figure 7 (*c*), where the maxima associated with higher harmonics have been completely obliterated at some values of y. A second observation is the tendency, at a given value of x, for the central and lower portions of the layer to exhibit greater irregularity than the upper portion ('filling in' of the frequency spectrum) of the layer. This is evident in figure 7 (*a*), (*b*), and (*c*) but is again most obvious in (*c*).

3.4. *Vertical amplitude distribution of spectral components*

Figure 10 (*a*) to (*h*) gives the variation of amplitude (and phase in some cases) across the shear layer for the various frequency components observed to be significant. Here again the forced data are presented, but data taken without forcing were similar in all important respects. The amplitude of the root-mean-square longitudinal velocity fluctuation is given in ft./sec, as a function of y, for different values of x/λ. The filled symbols represent values taken from the spectra measurements. These values give a good indication of the repeatability of the data, because the spectra were recorded with several hot wires over a period of days. The relative error within a single traverse is considerably smaller. No correction for hot-wire non-linearity was made.

For $x = 0{\cdot}2\lambda$, $0{\cdot}6\lambda$, and $0{\cdot}8\lambda$, the phase variation of the primary oscillation is presented. Since only the phase change across the shear layer is important, the phase angle, ϕ, was arbitrarily taken to be zero at the point where the slope of the phase curve was greatest. At $x = 0{\cdot}2\lambda$ and $0{\cdot}6\lambda$, several independent phase

measurements give an indication of the reliability of the data. For larger values of x/λ, where the subharmonic frequency is present, it is felt that the phase measurements are not sufficiently accurate to be presented.

One notices the large phase changes associated with the primary oscillation (a phase change of 180 degrees indicates a reversal of the direction of the longitudinal fluctuation), and some symmetry of shape about the point of maximum phase change. At $x = 1{\cdot}2\lambda$, the subharmonic first appears and grows rapidly until it eventually becomes the dominant component. The amplitude distributions spread vertically in the shear layer, so that the points of maximum amplitude of the primary and subharmonic components tend to move away from the region of high mean shear as x/λ increases. Between $x = 2{\cdot}4\lambda$ and $x = 3{\cdot}2\lambda$, there is a significant upward shift in the location of the point of maximum amplitude of the subharmonic component. At $x = 2{\cdot}4\lambda$, the maximum amplitude occurs at a point where $U/U_\delta = 0{\cdot}78$; while at $x = 3{\cdot}2\lambda$ the maximum amplitude of the subharmonic has moved upward to $U/U_\delta = 1{\cdot}0$. Notice also the tendency for the maxima and minima of the primary and subharmonic components to be reflected in the amplitude distributions of the higher harmonics.

3.5. *Wave speeds*

Figure 11 gives values of the wave (phase) speeds for both the primary and the subharmonic components as functions of vertical position in the shear layer. The wave speeds, C_r, were calculated from photographs of oscilloscope traces. The scatter in the measurements is large—especially for the subharmonic component. The wave speed of the primary oscillation is

$$C_r/U_0 = 0{\cdot}58 \pm 0{\cdot}11,$$

and the wavelength is $\lambda = 1{\cdot}25 \pm 0{\cdot}25$ in.

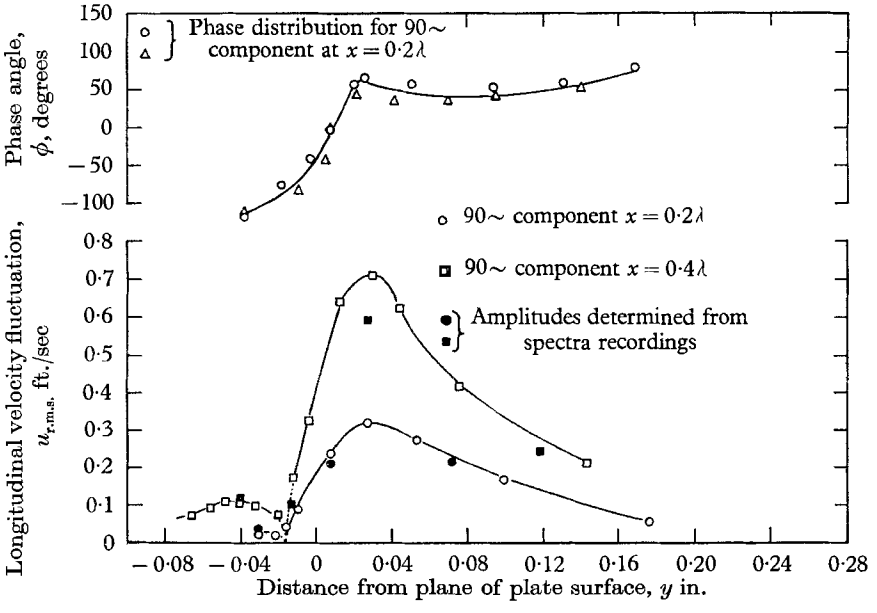

FIGURE 10. (*a*) Amplitude distribution of primary oscillation at $x = 0{\cdot}2\lambda$ and $x = 0{\cdot}4\lambda$. Phase distribution of primary oscillation at $x = 0{\cdot}2\lambda$.

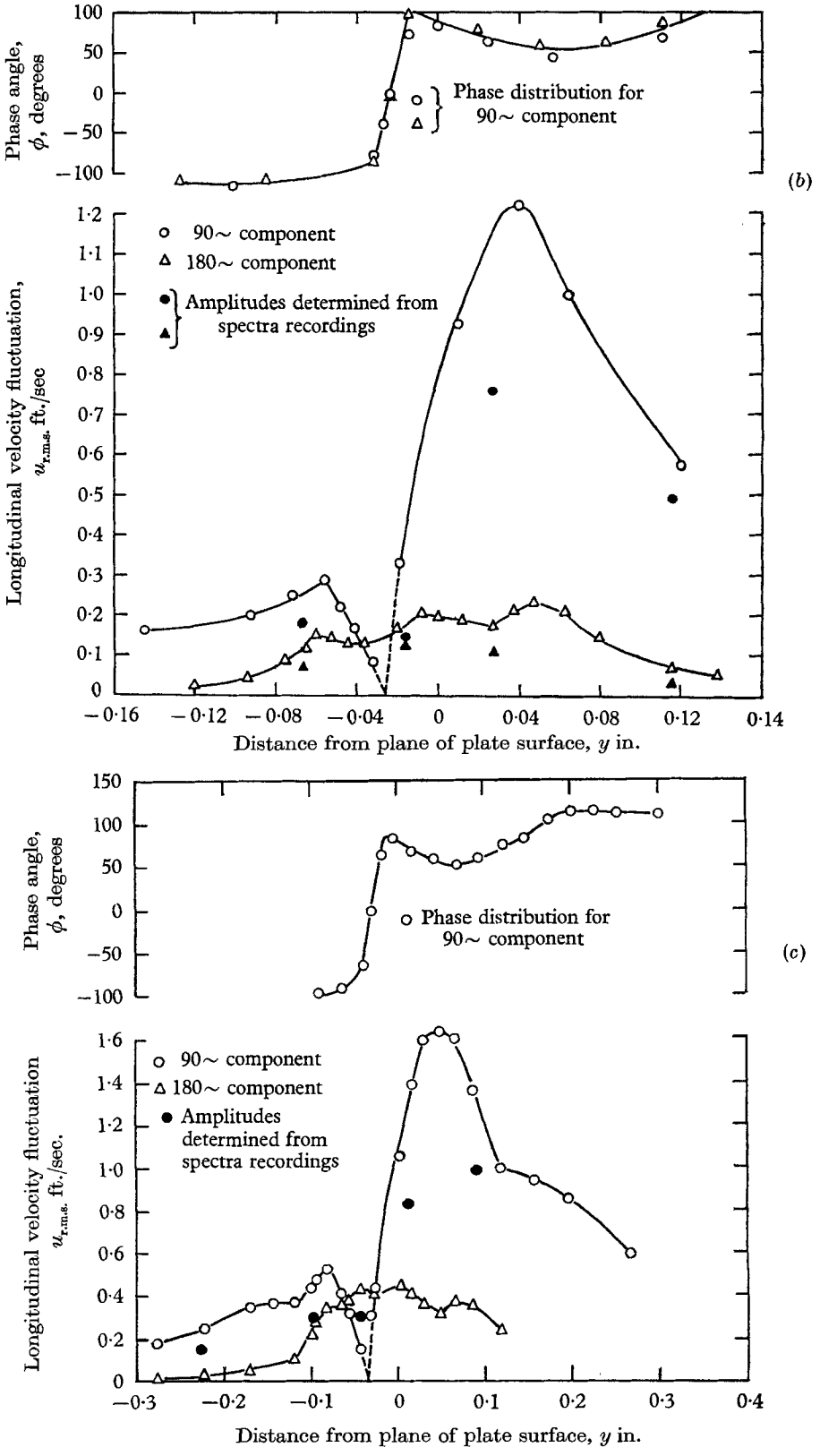

FIGURE 10. Amplitude distribution of the primary oscillation and the first harmonic at (*b*) $x = 0{\cdot}6\lambda$; (*c*) $x = 0{\cdot}8\lambda$. Phase distribution of the primary oscillation.

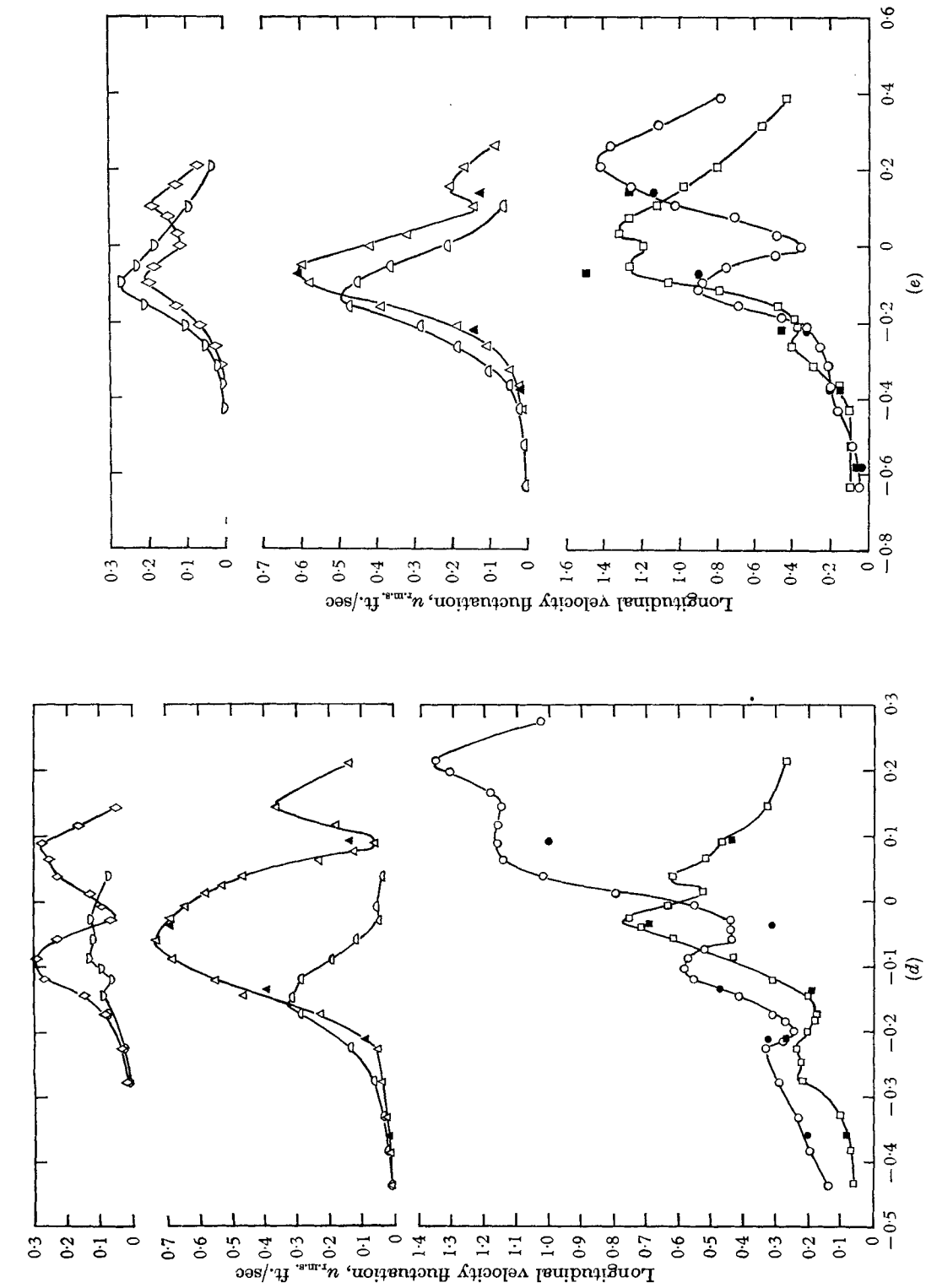

FIGURE 10. Amplitude distribution of various spectral components at (*d*) $x = 1{\cdot}2\lambda$; (*e*) $x = 1{\cdot}6\lambda$; (*f*) $x = 2{\cdot}0\lambda$; (*g*) $x = 2{\cdot}4\lambda$. □, 45 c/s component; ○, 90 c/s component; ⌓, 135 c/s; △, 180 c/s; ▽, 225 c/s; ◇, 270 c/s; ■, ●, ▲, amplitudes determined from spectra recordings.

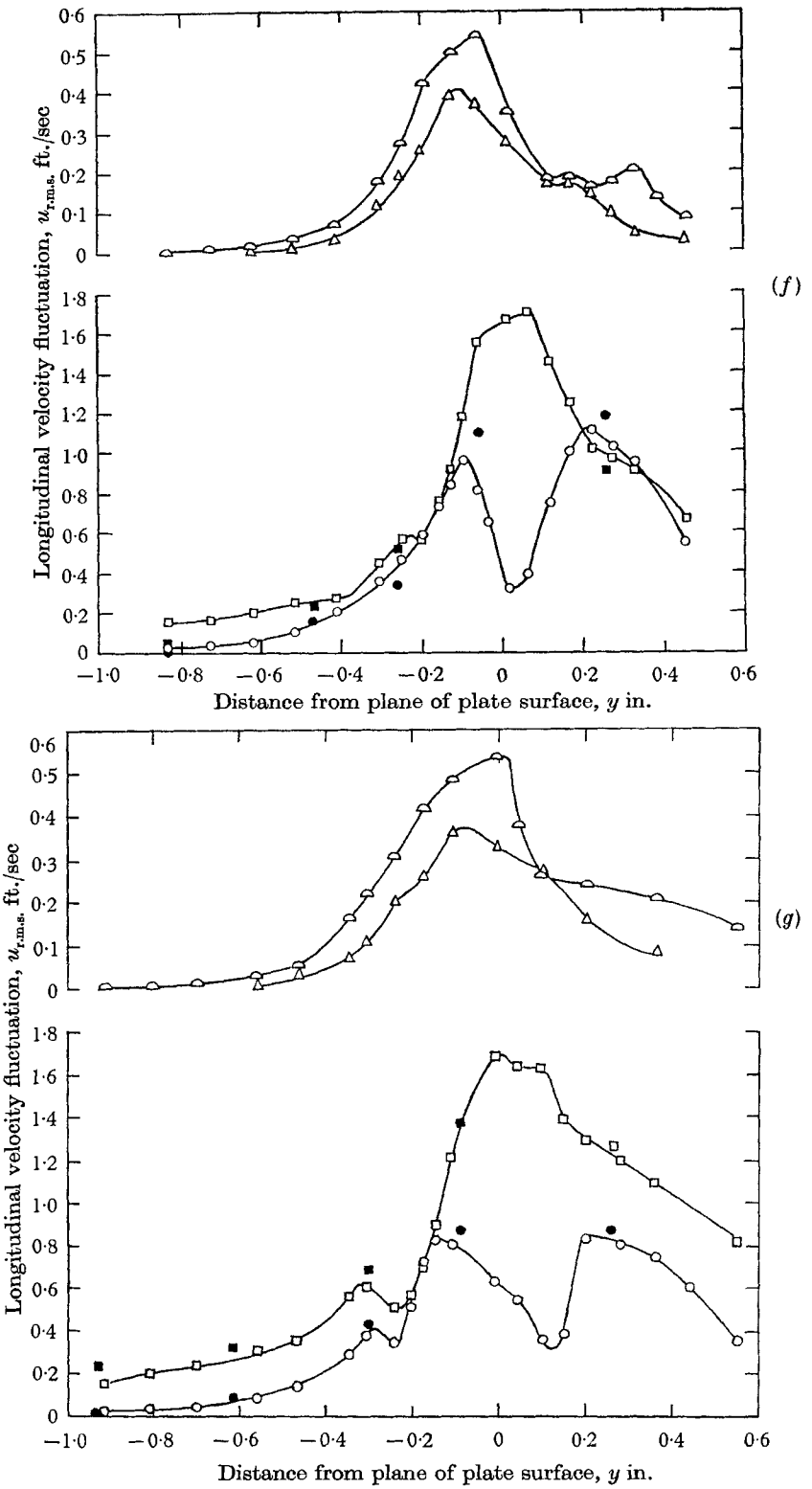

For legend see p. 295.

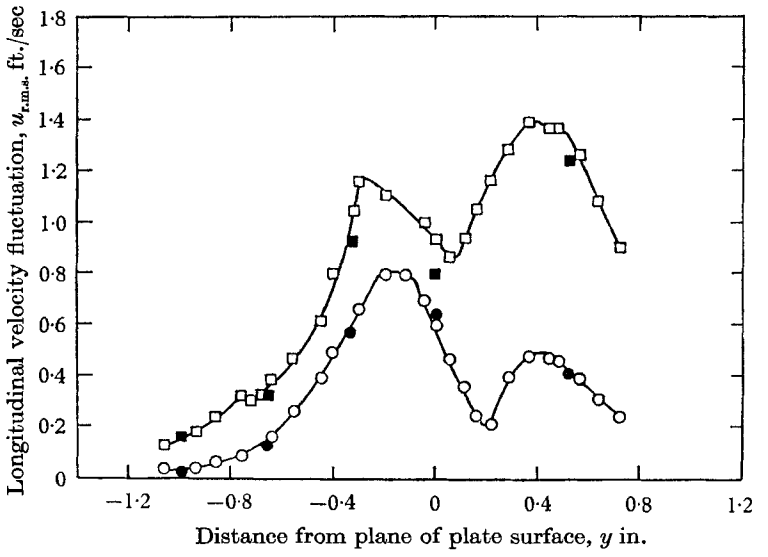

FIGURE 10. (*h*) Amplitude distribution of primary and subharmonic oscillations at $x = 3{\cdot}2\lambda$. □, 45 c/s component; 0·90 c/s; ■, ●, amplitudes determined from spectra recordings

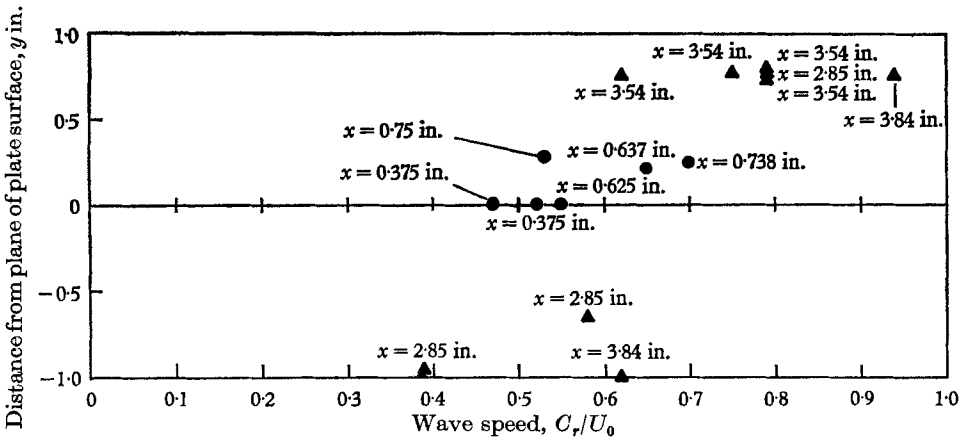

FIGURE 11. Wave speeds of the primary and subharmonic components at various vertical locations in the shear layer. ●, 90 c/s component; ▲, 45 c/s component.

The most significant feature is that the wave speed of the subharmonic component seems to be larger in the upper portion of the shear layer than in the lower portion.

3.6. *Intermittency*

During the course of the experiment it was evident by observing the instantaneous hot-wire traces that a strong intermittency was associated with the growth of the subharmonic component. The subharmonic oscillation was not present at all times, but disappeared completely at certain times. This intermittency was definitely associated with the subharmonic growth, since it was not observed in the primary oscillation upstream of the point where the subharmonic first appeared. The intermittency was correlated in the upper and lower portions

of the shear layer in the following manner. Figure 12 (*a*), (*b*) (plate 1) presents photographs which show the instantaneous wire voltages from two hot wires—one placed in the upper portion of the layer and one placed in the lower portion. The prevalent frequency is the 45 c/s component. At certain instants, the 45-cycle component is absent in the upper portion of the shear layer, but the 90-cycle component is present (although at a much reduced amplitude). At the same instant, the 45-cycle component is weak in the lower portion of the shear layer, and the signal is undefined.

3.7. *Bursting*

In some portions of the shear layer, the instantaneous wave forms exhibit characteristics which are similar to the bursts associated with the secondary breakdown in boundary-layer transition. Figure 13 (plate 2) presents several photographs of this phenomenon. As a comparison, a photograph of the secondary breakdown observed by Klebanoff *et al.* (1962) is reproduced. In the photograph reproduced from Klebanoff *et al.* decreasing velocity is in the downward direction; while, in the photographs taken in the shear layer, decreasing velocity is in the upward direction. The amplitudes of the bursts are much smaller, comparatively, in the present investigation than in the boundary-layer flow, so it may be misleading to use the term 'burst' when referring to the phenomenon observed in the shear layer.

Whether or not the term 'bursting' is used, the important point is that the phenomenon may arise from a secondary instability. The high-frequency 'bursts' always appear in conjunction with the subharmonic component of the primary oscillation and always occur at a definite point in the cycle. They occur in a portion of the shear layer where the subharmonic is well defined—about three wavelengths downstream and at the upper edge of the layer. From examination of the photographs, the frequency of the 'bursts' seems to be in the neighbourhood of 400–700 c/s, and the vertical extent is about 0·040 in.

3.8. *Three-dimensionality*

The measurements which were made to indicate the existence of spanwise structure were limited in extent. The tentative conclusion is that no significant spanwise structure exists whichis of comparable wave-length to the primary oscillation. (Periodic spanwise variations with a wavelength much longer than four inches would probably be difficult to detect in this investigation.) Mean profile traverses were recorded at $x = 0{\cdot}2\lambda$ and $x = 1{\cdot}2\lambda$, for spanwise locations, $z = 0$, $0{\cdot}4\lambda$, $0{\cdot}8\lambda$, and $1{\cdot}6\lambda$. None of these profiles showed noticeable differences. The 90-cycle component of the instantaneous hot-wire voltage was recorded as a continuous function of z (from $z = 0$ to $z = 1{\cdot}8\lambda$) for $x = 0{\cdot}2\lambda$, $y = -0{\cdot}084$ in.; and for $x = 1{\cdot}2\lambda$, $y = -0{\cdot}437$ in. The 45-cycle component of the instantaneous hot-wire voltage was recorded as a continuous function of z for several values of y at $x = 2{\cdot}4\lambda$. None of these measurements indicated any periodic spanwise variation.

The spanwise phase variation of the 90-cycle component was also recorded. While no periodic spanwise structure was evident, there was a departure from

two-dimensionality at the larger values of x/λ. The departure is probably a result of pre-existing variations in the incident stream rather than an inherent feature of the instability.

4. Discussion

4.1. *Growth of disturbances*

Figure 14 shows the maximum amplitudes of various spectral components as a function of x/λ. There is a region, at small values of x/λ, where the primary oscillation grows exponentially as predicted by linear stability theory. Deviation from exponential growth first occurs at about $x = 0{\cdot}4\lambda$ and at a value of $u_{\text{r.m.s.}}/U_0$ of about 5%. Downstream of $x = 0{\cdot}4\lambda$, in what could be called the non-linear region, the primary oscillation grows more slowly and eventually decreases. Other harmonic components are present in this region, but the maximum amplitudes are never more than about 11% of the freestream velocity. This agrees with the notion of a limiting amplitude for such disturbances (see Stuart 1960 and Schade 1964), although this work was performed in connexion with higher harmonics only. Schade (1964) has estimated a limiting amplitude for the case of a hyperbolic tangent profile, and has also given an estimate of the amplitude at which linear theory ceases to be a good approximation. These limiting amplitude results, including some taken from other investigations, are summarized in the following table:

	This investigation	2-d jet Sato (1960)	Boundary layer Klebanoff *et al.* (1962)	Theoretical estimate for tanh profile Schade (1964)	Circular cylinder Kovasznay (1949)
Linearity limit	5%	4%	2%	4%	—
Maximum amplitude	11%	10–20%	16%	17%	14%

4.2. *The linear region*

The initial wave growth observed in this experiment agrees closely with the more extensive results of Sato (1959). Although the linear region was not the primary concern, a brief summary will be given for the sake of completeness.

Using inviscid, linear stability theory, Lessen & Fox (1955) calculated the eigenvalues for unstable waves which could grow in a laminar shear layer between parallel streams. Sato (1959) compared the eigenvalues obtained experimentally with the eigenvalues calculated by Lessen & Fox. He was able to show that the initial oscillation which was observed to grow 'naturally' in the shear layer coincided with the theoretical oscillation having the maximum amplification rate. However, there was one important discrepancy. The amplitude distribution of the most unstable wave (obtained experimentally) was different from any of the calculated eigenfunctions (Sato 1959; Michalke 1964); and, furthermore, the distribution was difficult to reconcile with existing physical arguments (Lin 1955). (The distribution lacks any symmetry about the point of maximum mean vorticity.)

Gaster (1965) and Michalke (1966) have shed considerable light on this discrepancy by considering, theoretically, waves with spatial amplification rather than temporal amplification. (The case of spatial amplification agrees more closely with the experimental situation.) For a hyperbolic tangent velocity profile, Michalke (1966) found that the wave speed and frequency of the wave with maximum amplification was nearly identical for spatial and temporal growth; but the amplification rate and eigenfunction were different. There is good agreement between the present experimental results in the linear region and the calculations of Michalke (1966).

4.3. *The non-linear region*

(*a*) *Periodic spanwise structure*

In the region between $x = 0{\cdot}4\lambda$ and $x = 1{\cdot}2\lambda$, some interesting non-linear effects are observed. They include warping of the mean profile, the growth of harmonic components, the remarkable growth of the subharmonic component, and a very noticeable intermittency in the subharmonic oscillation. One effect which is notably absent, however, is the existence of periodic spanwise structure.

The question of periodic spanwise structure in two-dimensional unbounded flows is still unsettled. Early investigators such as Roshko (1954) and Hama, Long & Hegarty (1957) seem to have observed such structure. Roshko observed spanwise periodicity of very long wavelength ($\lambda = 18$ diameters) in the wake of a circular cylinder at low Reynolds number. Hama *et al.* observed periodic spanwise structure in the flow over a rearward-facing step at low Reynolds number. On the other hand, many recent investigators have not observed such structure. Tritton (1959) observed gradual spanwise warping in the wake of a cylinder, but no definite periodicity. This conclusion is supported by Bloor (1964) for cylinder wake measurements and by Sato & Kuriki (1961) for measurements in the wake of a thin flat plate. Periodic spanwise structure was not present (or of such a long wavelength as to be unimportant) in this investigation—at least up to $x = 1{\cdot}2\lambda$. Whether periodic structure exists downstream of this point is not known. The fact remains, though, that significant non-linear behaviour is observed in a region where the disturbance is essentially two dimensional.

(*b*) *Subharmonic growth*

Several notable features accompanied the subharmonic growth. First, the flow was essentially two dimensional (within the accuracy of the observations) before subharmonic generation. Secondly, the maximum amplitude of the primary oscillation decreased as the amplitude of the subharmonic oscillation increased (see figure 14). Thirdly, the subharmonic was noticeably intermittent; and, fourthly, the wave speed of the subharmonic was larger in the upper portion of the shear layer than in the lower portion.

A division of the primary wave disturbance seems to be occurring in the initial stage of subharmonic growth. A portion of the wave train moves upward and is convected at a higher velocity, and a portion moves downward with a decrease in velocity. Whatever interaction causes this division, it is evidently intermittent.

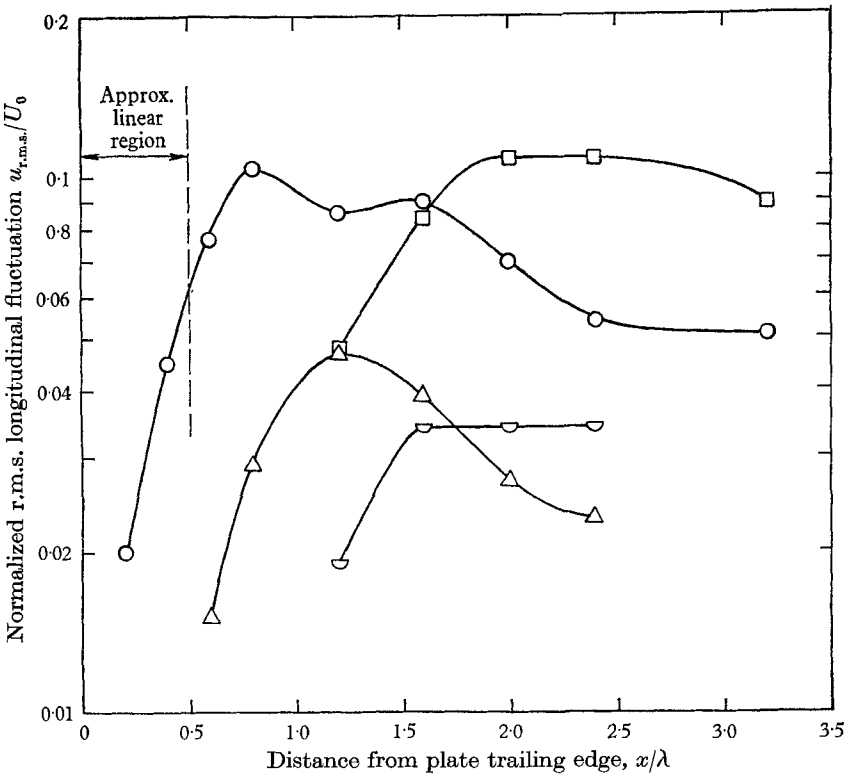

FIGURE 14. Maximum amplitudes of various spectral components as a function of downstream position. ○, Primary oscillation, 90 c/s maximum amplitude; □, subharmonic oscillation, 45 c/s maximum amplitude; △, second harmonic, 180 c/s maximum amplitude; ⌓, third harmonic of subharmonic, 135 c/s maximum amplitude.

Other wake flows which appear qualitatively similar, such as the flat plate wake and the two-dimensional jet (at low Reynolds numbers), do not exhibit such subharmonic response. Subharmonic growth apparently requires antisymmetry of the mean shear about the point where the primary oscillation originates. Subharmonic response arises most frequently as a result of parametric resonance, which is caused by the oscillatory nature of some physical parameter (Stoker 1950). This would lead one to suspect that another significant feature of the flow, with respect to subharmonic growth, is its periodic nature.

In a recent paper, Kelly (1965) examined the stability of a two-dimensional time-dependent shear flow composed of a hyperbolic tangent mean profile *plus* a finite amplitude oscillation representing the predicted primary oscillation. He showed that an oscillation with twice the wavelength of the original oscillatory flow can occur (for the case of temporal growth, at least); and, furthermore, that this is the only oscillation which is significantly amplified. Kelly also predicted that the growth rate of the subharmonic oscillation could exceed the growth rate of the primary oscillation when the amplitude of the primary oscillation was about 12% of the velocity difference across the shear layer. A re-examination of figure 14 will show that this estimate is in remarkably good agreement with the present experimental results.

Another interesting conclusion is that the process of subharmonic resonance could reappear again in connexion with the (original) subharmonic oscillation. Figure 15 shows a portion of the frequency spectrum at two downstream locations, in a region where the original subharmonic (45 c/s) is the dominant oscillation. There is a small but unmistakable peak at 22·5 c/s.

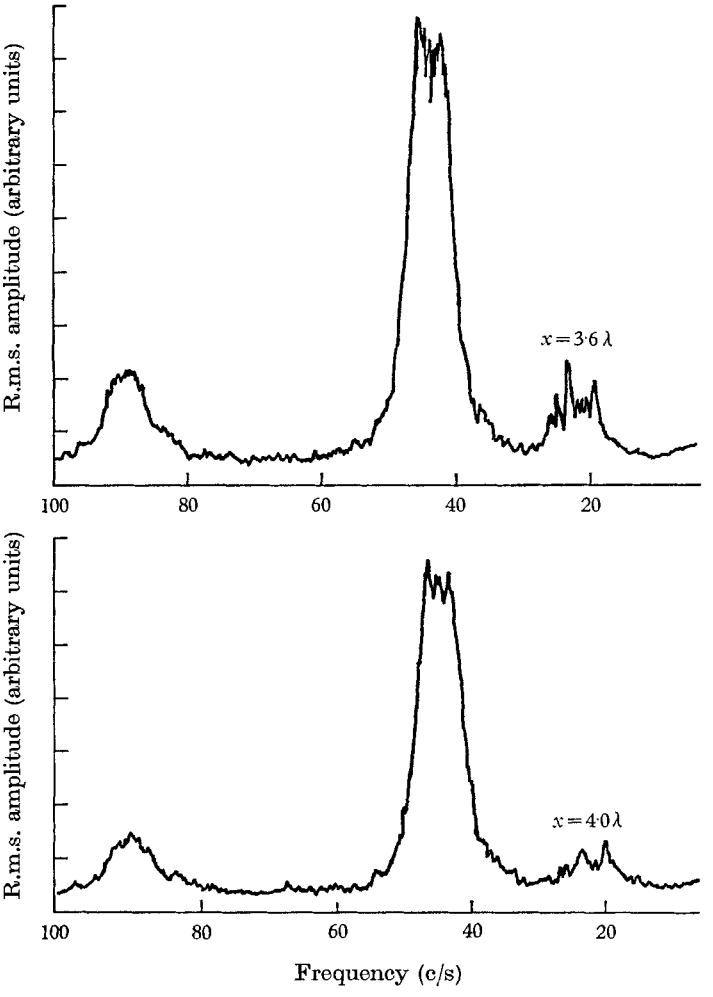

FIGURE 15. Several frequency spectra illustrating existence of a frequency component at 22·5 c/s.

(*c*) *Secondary instability*

Spectra measurements (§ 3.3) indicated that considerable irregularity was associated with the lower portions of the shear layer before such irregularity was found in the upper portions. To understand how this effect might originate, it is helpful to examine an instantaneous velocity profile. Figure 16 (*a*), (*b*), shows the instantaneous longitudinal velocity fluctuation at two downstream locations. These instantaneous fluctuations were determined from the measured mean-square amplitude and phase distributions of the primary oscillation. At $x = 0{\cdot}8\lambda$,

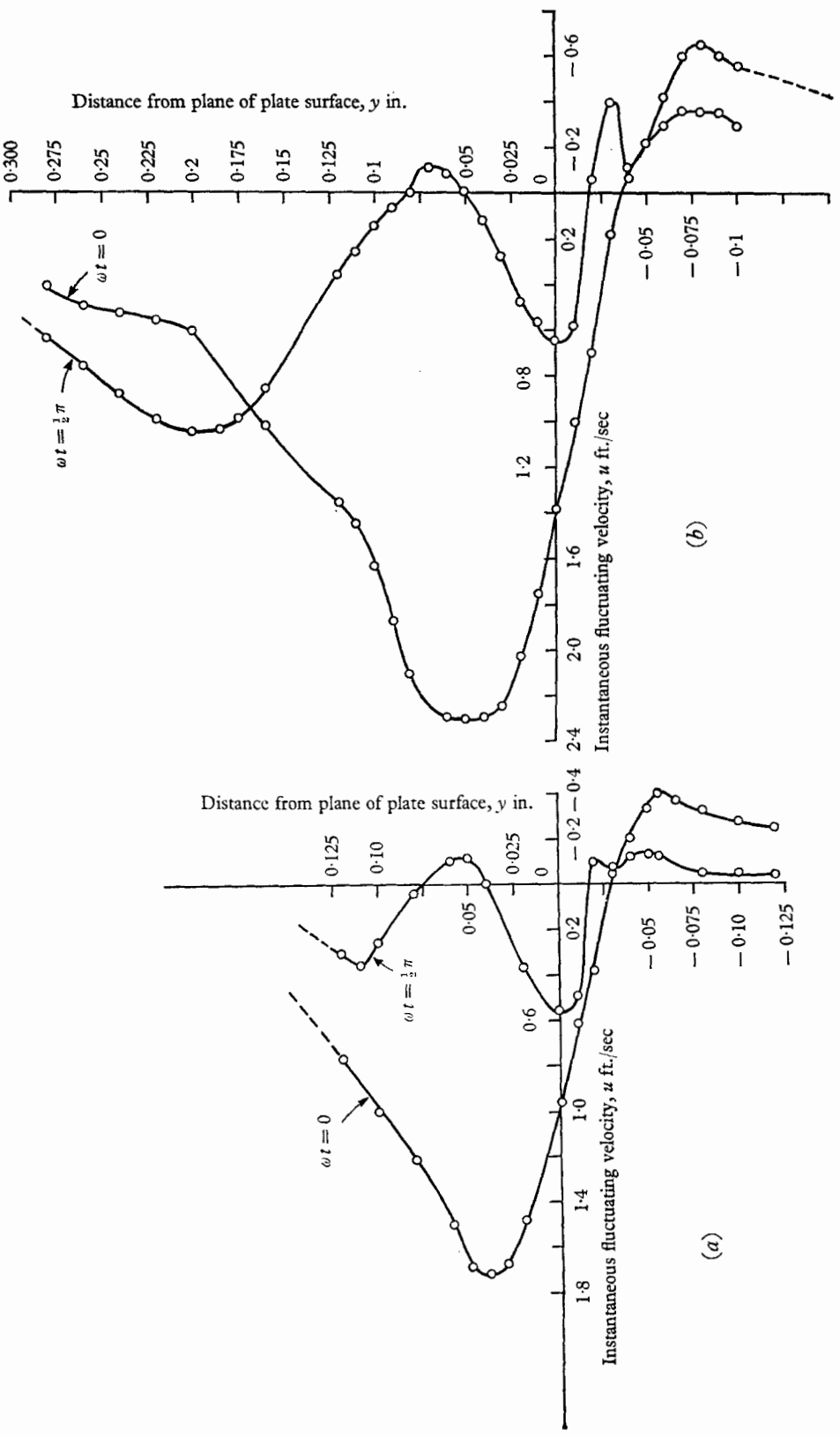

FIGURE 16. Instantaneous velocity fluctuation at quarter-cycle intervals. (*a*) $x = 0{\cdot}6\,\lambda$. Time, $t = 0$, is the instant when the maximum amplitude occurs at $y = 0{\cdot}04$ in. (*b*) $x = 0{\cdot}8\,\lambda$. Time, $t = 0$, is the instant of maximum amplitude at $y = 0{\cdot}05$ in.

the instantaneous velocity profile, figure 17, was constructed by a superposition of the mean velocity and the instantaneous fluctuation. (The instantaneous profile is only approximately correct because harmonic components other than the primary oscillation were neglected in the superposition.)

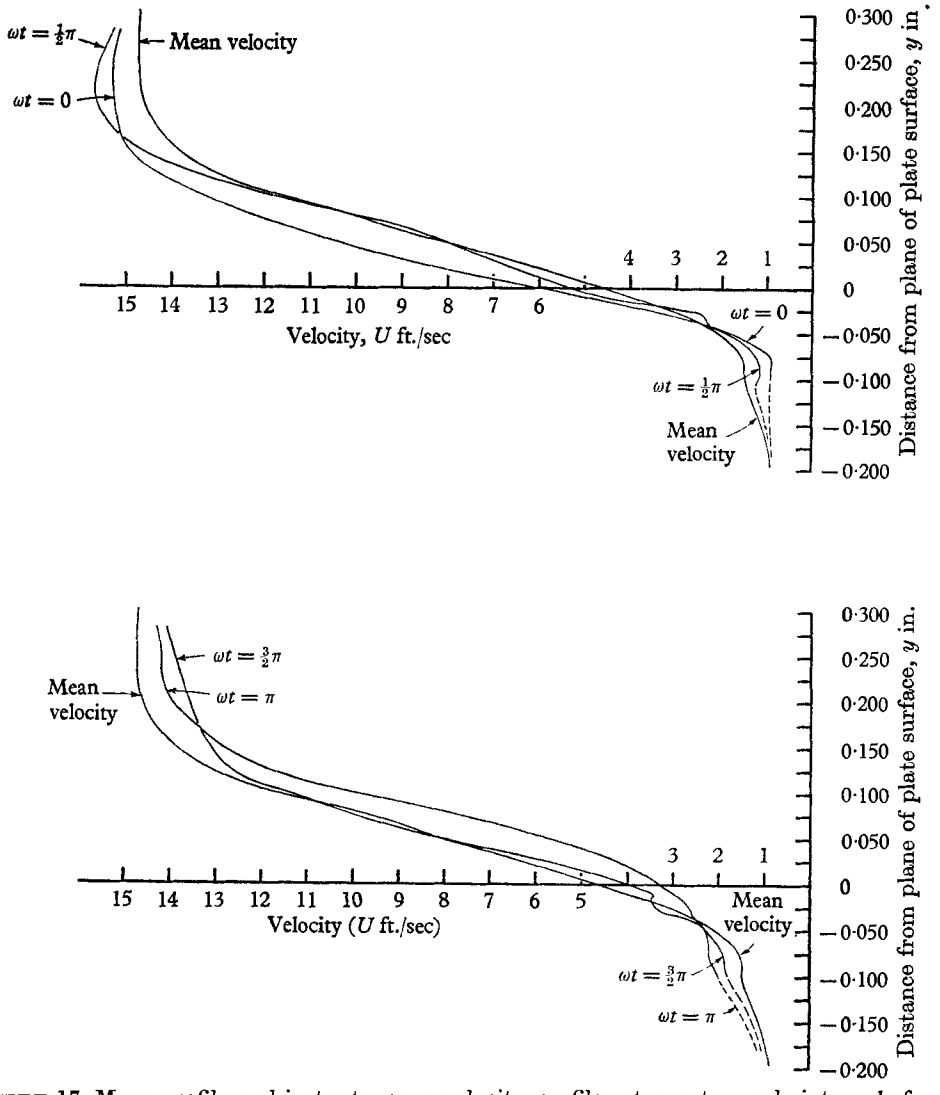

FIGURE 17. Mean profile and instantaneous velocity profiles at quarter-cycle intervals for $x = 0{\cdot}8\,\lambda$. Time, $t = 0$, is the instant of maximum amplitude at $y = 0{\cdot}05$ in.

A noticeable feature of the instantaneous profiles at $x = 0{\cdot}8\lambda$ is the extreme distortion in the region below the point of maximum mean shear. This distortion occurs in connexion with the rapid phase and amplitude variations of the primary oscillation, and produces profiles with one or more additional inflexion points. (Since these rapid variations are associated only with the primary oscillation at $x = 0{\cdot}8\lambda$, the neglect of harmonic content is not expected to change the qualitative features of the instantaneous profile.) The generation of profiles which have

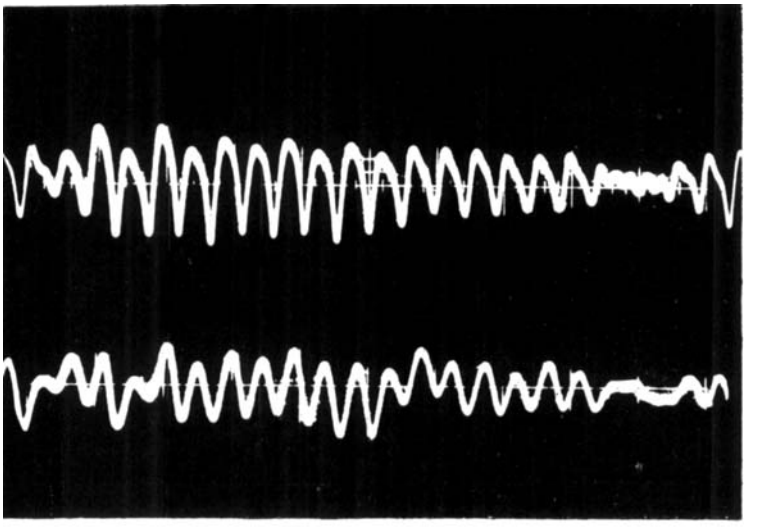

(*a*)

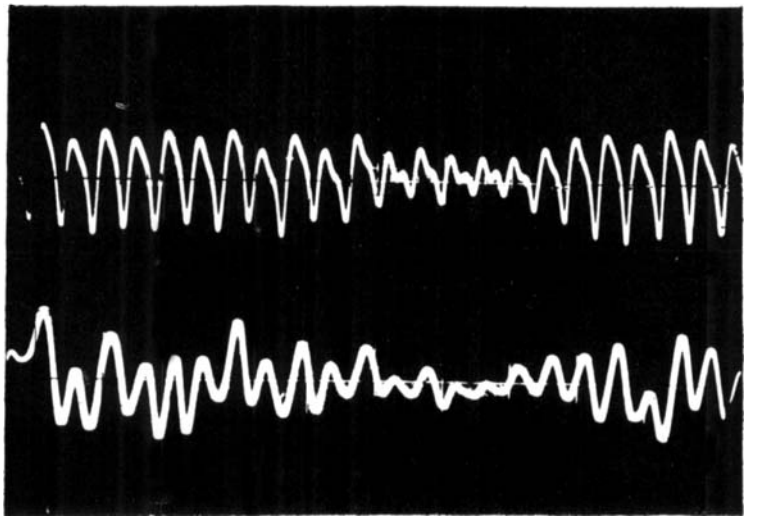

(*b*)

FIGURE 12. Instantaneous hot-wire traces illustrating correlation of intermittency of the subharmonic component. Top trace, hot wire at upper edge of shear layer; lower trace, hot wire at lower edge of shear layer.

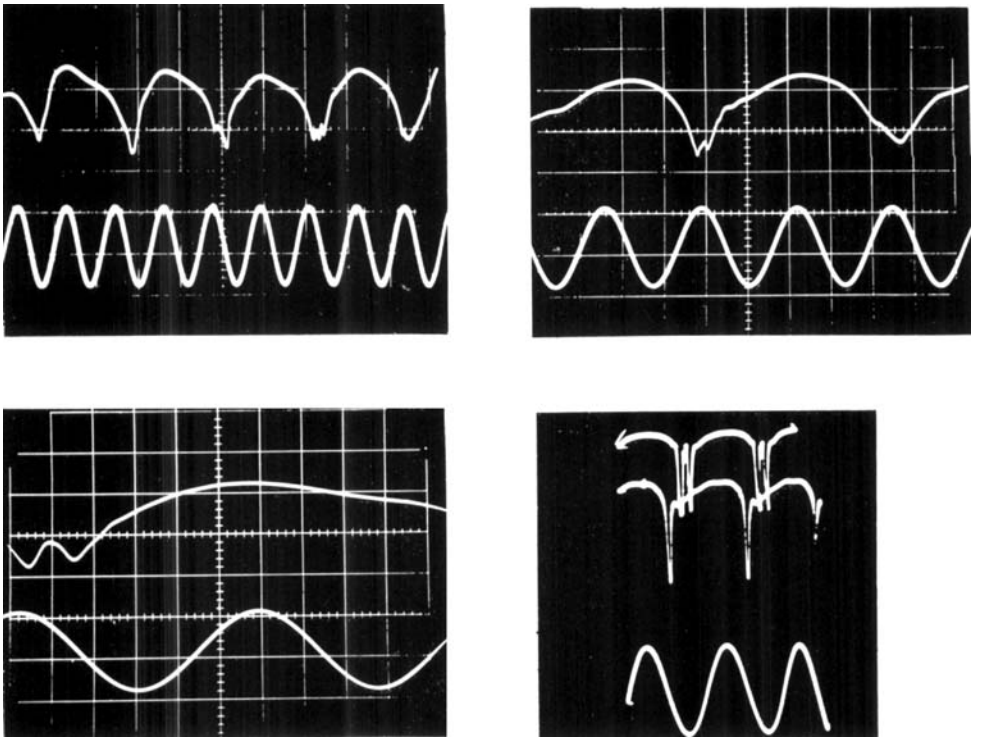

FIGURE 13. Instantaneous hot-wire traces illustrating a possible secondary instability. Upper trace, hot-wire signal; lower trace, 90-cycle speaker oscillation.

additional inflexion points and which appear roughly steady when moving with the wave, might be expected to produce additional instabilities just as the original instability was generated. The title, secondary instability, was given to this phenomenon by Klebanoff *et al.* (1962). It is not too surprising, then, that frequency smoothing between harmonic components and an increasing occurrence of higher frequencies is first associated with this region.

Photographic evidence was also given in figure 13 (plate 2) which suggests the presence of a secondary instability in the upper portion of the shear layer about three wavelengths downstream. In this connexion, it is interesting to notice the tendency for an inflexion point to form at the upper edge of the shear layer (figure 17, note $\omega t = \frac{1}{2}$). This tendency arises because a large change in the amplitude of the oscillation occurs in a region where the mean velocity is approaching the free-stream value. Apparently the maximum in the local shear produced in this region is not sufficient to cause an observable secondary instability. But one could imagine a much stronger local maximum being produced by an oscillation of larger amplitude moving upward into the region of constant mean velocity. This is exactly what occurs further downstream in connexion with the subharmonic component (see figure 10 (*g*), (*h*), and p. 293). Unfortunately, the instantaneous velocity profiles could not be determined in this region because the phase of the subharmonic component was not measured. However, the evidence seems to indicate this to be the origin of a secondary instability observed in figure 13.

(*d*) *Three-dimensional effects*

It was seen in § 4.3 (*b*) that many of the features observed in the non-linear region could be explained by a purely two-dimensional mechanism. Obviously, if turbulence is to ensue, the flow must eventually become three dimensional. Whether the eventual three-dimensionality arises from some inherent process in the shear layer, or is left more or less to chance irregularities, cannot be answered at present. As mentioned earlier, the preponderance of recent evidence seems to indicate the lack of definite spanwise structure—a view which is supported by this investigation. Unfortunately, none of the present results justify a more definite conclusion.

However, although evidence shows that periodic spanwise structure is not necessary for subharmonic generation, it is possible that subharmonic growth produces spanwise irregularity. Remember that intermittency is observed to be a significant characteristic of subharmonic growth. It is unlikely that this intermittency is two-dimensional. Thus the mechanism which produces intermittency of the subharmonic component produces spanwise randomness (phase variation) as well. The high-frequency oscillations ascribed to secondary instability must be three dimensional also, simply because it is impossible to conceive that such a complicated, unsteady process could remain two dimensional.

4.4 *A summary of the instability process*

In the region nearest the plate, the primary oscillation, predicted by linear stability theory, grows rapidly and is accompanied by a gradual growth of higher harmonics. The large amplitude and rapid phase change associated with the

primary oscillation causes additional inflexion points to be formed in the instantaneous velocity profile. This behaviour indicates a strong possibility of a secondary instability eventually forming in the lower portion of the shear layer. Although this instability was not well-defined experimentally, the lower portion of the wake becomes irregular sooner than the upper portion.

When the maximum amplitude of the primary oscillation has reached about 10% of the free-stream velocity, the subharmonic of one-half frequency begins to grow, and the amplitude of the primary oscillation decreases slightly. The subharmonic growth is coincident with a warping of the mean velocity profile and a rapid decrease in the maximum mean shear. Subharmonic growth is also accompanied by the growth of harmonics of the subharmonic, so that as many as six discrete frequencies can be observed in this region. The subharmonic component is intermittent; and this intermittency is partly responsible for the eventual decay of the discrete spectrum.

When the amplitude of the subharmonic (now the dominant oscillation) reaches about 10% of the free-stream velocity, a secondary instability occurs in the upper portion of the shear layer. The frequency of this secondary instability is about ten times the frequency of the subharmonic.

No periodic spanwise structure seems to be present, although three-dimensional measurements were for the most part confined to the region upstream of $x = 1{\cdot}2\lambda$. The oscillations associated with the secondary instability must certainly be three dimensional, while the lower frequency components could develop random three-dimensional structure from the intermittent nature of the subharmonic oscillation.

Thus the process of instability is first to increase the number of important frequencies, from a single frequency, by the creation of both higher and lower harmonics. Then the spectrum is blurred by randomizing processes, and still higher frequencies are generated by secondary instabilities. These developments are accompanied by an increasingly random spanwise structure.

The author is most grateful to Professor Erik Mollo-Christensen for his many suggestions and continued encouragement. This work was supported by the National Aeronautics and Space Administration, Grants NsG-31-60 and NSG 496 and by the Office of Naval Research under Grant Nonr-1841(89).

REFERENCES

BENNEY, D. J. 1961 *J. Fluid Mech.* **10**, 209.
BETCHOV, R. & SZEWCZYK, A. 1963 *Phys. Fluids* **6**, 1391.
BLOOR, M. S. 1964 *J. Fluid Mech.* **19**, 290.
DRAZIN, P. G. & HOWARD, L. N. 1962 *J. Fluid Mech.* **14**, 257.
ESCH, R. E. 1957 *J. Fluid Mech.* **3**, 289.
FOOTE, J. R. & LIN, C. C. 1950 *Quart. Appl. Math.* **8**, 265.
GASTER, M. 1965 *J. Fluid Mech.* **22**, 433.
GREENSPAN, H. P. & BENNEY, D. J. 1963 *J. Fluid Mech.* **15**, 133.
HAMA, F. R., LONG, J. D. & HEGARTY, J. C. 1957 *J. Appl. Phys.* **28**, 388.
KELLY, R. E. 1965 *Nat. Phys. Lab. Aero Rep.* no. 1161.
KLEBANOFF, P. S., TIDSTROM, K. D. & SARGENT, L. M. 1962 *J. Fluid Mech.* **12**, 1.

KOVASZNAY, L. S. G. 1949 *Proc. Roy. Soc.* A, **198**, 174.

LESSEN, M. & FOX, J. A. 1955 *50 Jahre Grenzschichtforschung*, p. 122 (eds. H. Gortler and W. Tollmien). Braunschweig: Vieweg.

LIEPMANN, H. W. & LAUFER, J. 1947 *NACA TN* no. 1257.

LIN, C. C. 1953 *NACA TN* no. 2887.

LIN, C. C. 1955 *The Theory of Hydrodynamic Stability*. Cambridge University Press.

LOCKE, R. C. 1951 *Quart. J. Mech. Appl. Math.* **4**, pt. 1.

MICHALKE, A. 1964 *J. Fluid Mech.* **19**, 543.

MICHALKE, A. 1965 *J. Fluid Mech.* **22**, 371.

MICHALKE, A. 1966 To be published. *J. Fluid Mech.*

RAYLEIGH, LORD 1896 *The Theory of Sound*, volume II, 2nd ed. London: MacMillan.

ROSHKO, A. 1954 *NACA TR* no. 1191.

SATO, H. 1956 *J. Phys. Soc. Japan*, **11**, 702.

SATO, H. 1959 *J. Phys. Soc. Japan* **14**, 1797.

SATO, H. 1960 *J. Fluid Mech.* **7**, 53.

SATO, H. & KURIKI, K. 1961 *J. Fluid Mech.* **11**, 321.

SATO, H. & SAKAO, F. 1964 *J. Fluid Mech.* **20**, 337.

SCHADE, H. 1964 *Phys. Fluids* **7**, 623.

STOKER, J. J. 1950 *Nonlinear Vibrations*. New York: Interscience.

STUART, J. T. 1960 *J. Fluid Mech.* **9**, 353.

TATSUMI, T. & GOTOH, K. 1960 *J. Fluid Mech.* **7**, 433.

TRITTON, D. J. 1959 *J. Fluid Mech.* **6**, 547.

WEHRMANN, O. & WILLE, R. 1958 *Grenzschichtforschung, IUTAM-symposium*, Freiburg 1957, p. 387. Berlin: Springer.